Mesoscopic admittance of a double quantum dot

Audrey Cottet, Christophe Mora, and Takis Kontos

Laboratoire Pierre Aigrain, Ecole Normale Supérieure, CNRS (UMR 8551), Université P. et M. Curie, Université D. Diderot, 24 rue Lhomond, F-75231 Paris Cedex 05, France

We calculate the mesoscopic admittance $G(\omega)$ of a double quantum dot (DQD), which can be measured directly using microwave techniques. This quantity reveals spectroscopic information on the DQD and is also directly sensitive to a Pauli spin blockade effect. We then discuss the problem of a DQD coupled to a high quality photonic resonator. When the photon correlation functions can be developed along a random-phase-approximation-like scheme, the response of the resonator gives an access to $G(\omega)$.

The possibility to couple nanoconductors to capacitive gates has been instrumental for exploring electronic transport in these systems. Applying dc gate voltages allows one to tune the energies of localized electronic orbitals to perform the transport spectroscopy of a nanoconductor and reach various conduction regimes. Gates can also be coupled to ac electric fields, to obtain, e.g., photoassisted tunneling or charge pumping.[1] Recently, the mesoscopic admittance $G(\omega)$ of a single quantum dot subject to an ac gate voltage has been investigated experimentally.[2] The low-frequency limit $G(\omega \to 0) \simeq -i\omega C_{\mathrm{meso}}$ can be interpreted in terms of a mesoscopic capacitance C_{meso} determined by the circuit geometric capacitances but also by the dot energy spectrum, which sets the ability of the dot to absorb electrons. This problem has been discussed theoretically in the regimes of weak[3,4] and strong Coulomb interactions.[5,6] In a more quantum view, gates can mediate a coupling between the electrons of a nanocircuit and cavity photons. This is widely exploited in the context of circuit-quantum electrodynamics. Coupling superconducting qubits to a coplanar waveguide photonic resonator allows an efficient manipulation, coupling, and readout of the qubits.[7,8] In the dispersive regime where a qubit and a resonator are strongly detuned, the cavity photons experience a frequency shift which reveals the qubit state. This shift is sometimes discussed in terms of the qubit mesoscopic capacitance.[9] The resonant regime leads to vacuum Rabi oscillations in which the nanocircuit alternatively emits and reabsorbs a single photon.[10]

Double quantum dots (DQDs) are mesoscopic circuits which can be made out of, e.g., submicronic two-dimensional electron-gas structures,[11] or top-gated carbon nanotubes.[12] These devices can be used to elaborate various types of qubits,[11,13,14] and offer interesting possibilities in the context of circuit-quantum electrodynamics.[15,16] The behavior of a photonic resonator coupled to a DQD has been recently studied experimentally.[17] However, on the theoretical side, this problem has aroused little attention. Besides, the ac gate biasing of DQDs has been studied in the context of spin and charge pumping (see, e.g., Ref. 18 and references therein) and photoassisted dc transport (see, e.g., Ref. 19), but no theoretical study has been performed in the context of mesoscopic admittance measurements.

In the first part of this Rapid Communication, we calculate the mesoscopic admittance $G(\omega)$ of a DQD. We show that this quantity displays a very rich behavior. In particular, it is directly sensitive to a Pauli spin-blockade effect.[12,20] A

measurement of $G(\omega)$ seems an interesting way to perform the spectroscopy of a DQD, in the context of, e.g., a qubit use, which can forbid invasive dc probes.[16] In the second part of this Rapid Communication, we discuss the problem of a DQD weakly coupled to a high quality photonic resonator. The resonator could offer an alternative to direct ac gate biasing for measuring $G(\omega)$. When the photon correlation functions can be developed along a random-phase-approximation-like scheme, both the dispersive and resonant behaviors of the resonator can be predicted from $G(\omega)$. We briefly discuss the range of validity of the RPA scheme in the noninteracting limit.

We first discuss the mesoscopic admittance measurement [Figs. 1(a) and 1(b)]. We consider two single-orbital dots L and R with orbital energies ξ_L and ξ_R, coupled together through a spin-conserving tunnel barrier with a hopping constant t and a capacitance C_m. We note $\hat{c}_{d\sigma}$ the annihilation operator associated to an electron with spin $\sigma \in \{\uparrow, \downarrow\}$ on dot $d \in \{L,R\}$, $\hat{n}_{d\sigma} = \hat{c}_{d\sigma}^\dagger \hat{c}_{d\sigma}$, and $\hat{n}_d = \hat{n}_{d\uparrow} + \hat{n}_{d\downarrow}$. Dot d is connected through a tunnel contact to a grounded reservoir, and connected through a capacitance C_g^d [C_{ac}^d] to a dc [ac] bias generator with voltage V_g^d [$V_{\mathrm{ac}}(t)$]. The reservoir states are described by annihilation operators $\hat{c}_{dk\sigma}$. The full Hamiltonian of the circuit writes (up to a term proportional to the identity operator) $\hat{H}_1 = \hat{H}_{\mathrm{DQD}} + \hat{H}_l + \hat{H}_{\mathrm{ac}}$ with[21]

$$\hat{H}_{\mathrm{DQD}} = \sum_{d,\sigma}(\epsilon_d - \sigma[g\mu_B B/2])\hat{n}_{d\sigma} + \sum_d \hat{n}_d(\hat{n}_d - 1)E_c^d$$
$$+ U_m \hat{n}_L \hat{n}_R + t\sum_\sigma(\hat{c}_{L\sigma}^\dagger \hat{c}_{R\sigma} + \mathrm{H.c.}), \quad (1)$$

$$\hat{H}_l = \sum_{d,k,\sigma}([t_d \hat{c}_{d\sigma}^\dagger \hat{c}_{dk\sigma} + \mathrm{H.c.}] + \epsilon_{dk\sigma}\hat{c}_{dk\sigma}^\dagger \hat{c}_{dk\sigma}),$$
$$\hat{H}_{\mathrm{ac}}[V_{\mathrm{ac}}(t)] = \sum_d e\alpha_d \hat{n}_d V_{\mathrm{ac}}(t), \quad (2)$$

$\epsilon_{L(R)} = E_c^{L(R)}[1 - 2n_g^{L(R)} - 2n_g^{R(L)}(C_m/C_\Sigma^{R(L)})] + \xi_{L(R)}$, $n_g^d = C_g^d V_g^d/e$, and C_Σ^d is the total capacitance of dot d.[22] For later use, we define tunnel rates $\Gamma_d = \pi\nu_0|t_d|^2/\hbar$ to the leads, with ν_0 the density of states per spin for reservoir d. We note $\Delta A(t) = \langle \hat{A} - \langle\hat{A}\rangle_0\rangle$ with $\langle\hat{A}\rangle_0$ the average value of an operator $\hat{A}$ for $V_{\mathrm{ac}} = 0$. From the linear-response theory, one finds $\Delta n_d(\omega) = e[\alpha_L \chi_{d,L}(\omega) + \alpha_R \chi_{d,R}(\omega)]V_{\mathrm{ac}}(\omega)$ with charge correlation functions $\chi_{d,d'}(t) = -i\theta(t)\langle[\hat{n}_d(t),\hat{n}_{d'}]\rangle_0$. The charge of the capacitor plates connected to V_{ac} writes
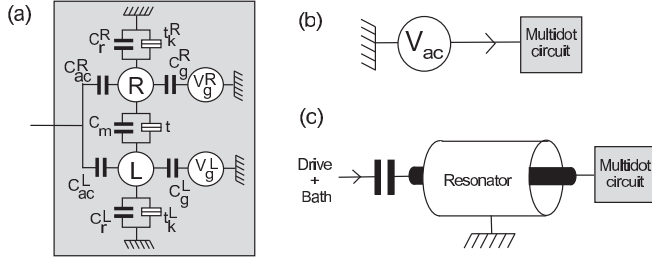
FIG. 1. (a) DQD circuit considered in this Rapid Communication. (b) Configuration used for the measurement of the DQD mesoscopic admittance. (c) Coupling scheme to a photonic resonator.

$\hat{Q}_{ac} = -\alpha_L \hat{n}_L e - \alpha_R \hat{n}_R e + 2\lambda_2 V_{ac}$. Therefore one obtains

$$\Delta Q_{ac}(\omega)/V_{ac}(\omega) = 2\lambda_2 - (e^2/\hbar)\Pi(\omega) = G(\omega)/(-i\omega) \quad (3)$$

with $\Pi(\omega) = \sum_{d,d'} \alpha_d \alpha_{d'} \chi_{d,d'}(\omega)$ and $G(\omega)$ the admittance of the DQD. The term in λ_2 corresponds to the DQD response for totally closed quantum dots (i.e., $t_d = t = 0$). In the low-frequency limit, i.e., ω much smaller than the characteristic energies involved in the DQD dynamics (including $\Gamma_{L(R)}$), we obtain $C_{meso} = 2\lambda_2 - (e^2/\hbar)\Pi(0) \in \mathbb{R}$. One can calculate $\Pi(0)$ from the definition of $\chi_{d,d'}(t)$. Alternatively, assuming that $\hat{n}_L$ and $\hat{n}_R$ have finite correlation times, i.e., $\lim_{t \to +\infty} \chi_{d,d'}(t) = 0$, one can use

$$\Pi(0) = \hbar \sum_{d,d'} \alpha_d \alpha_{d'} \partial \langle \hat{n}_d \rangle_0 / \partial \epsilon_{d'} \quad (4)$$

with, assuming that the eigenstates $|\psi_i\rangle$ of $\hat{H}_{DQD}$ (with energies E_i), are thermally populated,[19]

$$\langle \hat{n}_d \rangle_0 = \sum_i \langle \psi_i | \hat{n}_d | \psi_i \rangle \exp(-\beta E_i) / \sum_i \exp(-\beta E_i). \quad (5)$$

We first discuss the noninteracting limit, using $E_c^{L(R)}, U_m \to 0$, $C_m = 0$, $B = 0$, and $\Gamma_{L(R)} = \Gamma$, which yields $\epsilon_d = -C_g^d e V_g^d / C_\Sigma^d$. In this case, $\Pi(\omega)$ can be expressed exactly as $\Pi(\omega) = \Pi_1(\omega) + \Pi_2(\omega)$, with $\Pi_{1[2]}(\omega) = \sum_{s \in \{+,-\}} \Pi_{s,s[\bar{s}]}(\omega)$,

$$\Pi_{s,s'}(\omega) = \frac{4\hbar}{\pi} \int_{-\infty}^{+\infty} d\varepsilon \, \Gamma f(\varepsilon) g_{s,s'}(\omega) / [(\varepsilon - E_s)^2 + \Gamma^2] \quad (6)$$

and $g_{s,s'}(\omega) = \lambda_{s,s'}^2 (\varepsilon - E_{s'}) / [(\varepsilon - E_{s'})^2 - (\omega + i\Gamma)^2]$. Here, $\bar{s}$ denotes $-s$. We use $\lambda_{s,s} = \{\alpha_L + \alpha_R + s(\alpha_L - \alpha_R) \cos[\theta]\}/2$, $\lambda_{s,\bar{s}} = -(\alpha_L - \alpha_R) \sin[\theta]/2$, $\theta = \arctan[2t/(\epsilon_L - \epsilon_R)]$, $E_\pm = (\epsilon_L + \epsilon_R \pm \Delta_c)/2$, and $\Delta_c = \sqrt{(\epsilon_L - \epsilon_R)^2 + 4t^2}$. In the limit $T = 0$ and $\omega = 0$, we obtain $\Pi_1(0) = -2\hbar \sum_s \lambda_{s,s}^2 \nu_s$ with $\nu_s = \Gamma/\pi[E_s^2 + \Gamma^2]$ the DQD partial density of states (DOS) corresponding to state s dressed by the leads. This result is reminiscent from the noninteracting single quantum dot case[3,23] where the dot DOS plays a crucial role. The term $\Pi_2(\omega)$ is more specific to the DQD case and is not simply related to ν_s. It is finite when $\alpha_L \neq \alpha_R$, i.e., when V_{ac} induces different renormalizations of the levels ϵ_L and ϵ_R. Processes which involve electronic transfers between the two dots thus contribute crucially to $\Pi_2(\omega)$. We now focus on the limit $0 < \Gamma \ll k_B T \ll t$. At low frequencies, we obtain
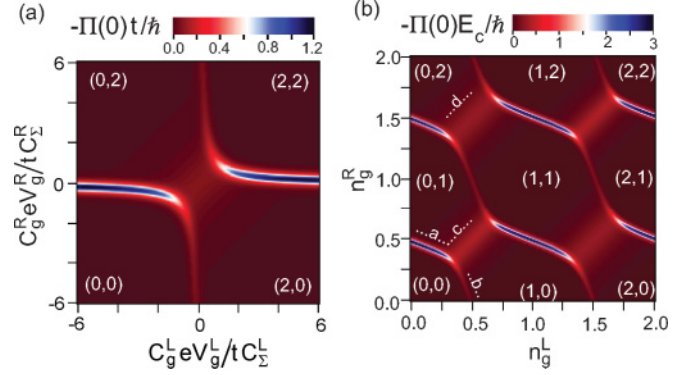

FIG. 2. (Color online) Response function $\Pi(0)$ versus the DQD gate voltages in the noninteracting/interacting cases [panels (a)/(b)]. The white numbers indicate the DQD most stable charge states (Ref. 24). We have used $\alpha_L = -0.1$, $\alpha_R = -0.5$, and $B = 0$. In panel (a) we have used $k_B T/t = 0.1$. In panel (b) we have used $E_c^{L(R)} = E_c$, $U_m = 0.7E_c$, $t = 0.1E_c$, and $k_B T = 0.02E_c$.

from Eq. (6)

$$\Pi_1(0) = -\beta\hbar \sum_s \lambda_{s,s}^2 \cosh^{-2}[\beta E_s/2]/2, \quad (7)$$

$$\Pi_2(0) = -4\hbar(\alpha_L - \alpha_R)^2 t^2 [f(E_-) - f(E_+)]/\Delta_c^3 \quad (8)$$

with $f(\varepsilon) = 1/[1 + \exp(\beta\varepsilon)]$. These results can also be obtained from Eqs. (4) and (5). Hence $\Pi(0)$ does not depend anymore on Γ. Figure 2(a) shows $\Pi(0)$ versus the DQD gate voltages. The weak resonant line crossing the $V_g^L = V_g^R = 0$ point is due to $\Pi_2(0)$ while the anti-crossing lines are due to $\Pi_1(0)$. For $\omega, 2t \gg \Gamma$, we obtain $\Pi(\omega) \simeq \Pi_2(\omega)$ with $\Pi_2(\omega) \simeq 4\hbar(\alpha_L - \alpha_R)^2 t^2 [f(E_-) - f(E_+)]/\Delta_c(\omega^2 - \Delta_c^2)$. Dot/lead electron transfers are not relevant anymore because they are too slow, and $\Pi(\omega)$ shows a resonant behavior due to the internal dynamics of the DQD.

We now discuss the interacting case for $0 < \Gamma_{L(R)} \ll k_B T \ll t \ll E_c^{L(R)}, U_m$. The DQD stability diagram corresponds to the standard honeycomb pattern.[21] Figure 2b shows the variations of $\Pi(0)$ with $n_g^{L(R)}$, calculated from Eqs. (4) and (5) for $B = 0$. Different kinds of resonant lines occur in this graph. The first kind corresponds to electron transfers between the DQD and a lead, and has a width set by T. For instance, line a corresponds to transitions between states $(0,0)$ and $(0,\sigma)$, with $\sigma \in \{\uparrow, \downarrow\}$.[24] This line can be approximated (away from triple points) as $\Pi(0) \simeq -\hbar\alpha_R^2 \beta/4 \cosh^2[\beta\epsilon_R/2]$, which is reminiscent from Eq. (7). Similarly, line b corresponds to $\Pi(0) \simeq -\hbar\alpha_L^2 \beta/4 \cosh^2[\beta\epsilon_L/2]$. The second kind of resonances corresponds to electron transfers between the two dots, in the same $\hat{n}_R + \hat{n}_L$ subspace. For instance, line c involves resonances between DQD states $(\sigma, 0)$ and $(0, \sigma)$, with $\sigma \in \{\uparrow, \downarrow\}$. It can be approximated by $\Pi(0) \simeq -2\hbar(\alpha_L - \alpha_R)^2 t^2/\Delta_c^3$, which recalls Eq. (8). Line d corresponds to a resonance between $(0, \uparrow\downarrow)$, $(\uparrow, \downarrow)$ and $(\downarrow, \uparrow)$. It can be approximated by $\Pi(0) \simeq -4\hbar(\alpha_L - \alpha_R)^2 t^2/\Delta_d^3$ with $\Delta_d = \sqrt{(E_{02} - E_{11})^2 + 8t^2}$ and $E_{02} - E_{11} = \epsilon_R - \epsilon_L + 2E_c^R - U_m$. The above expressions again do not involve the values of the tunnel rates due to $\Gamma_{L(R)} \ll k_B T$. Along line c, $\Pi(0)$ reaches a maximum which is $\sqrt{2}$ higher than along line d, because lines c and d involve resonances between a
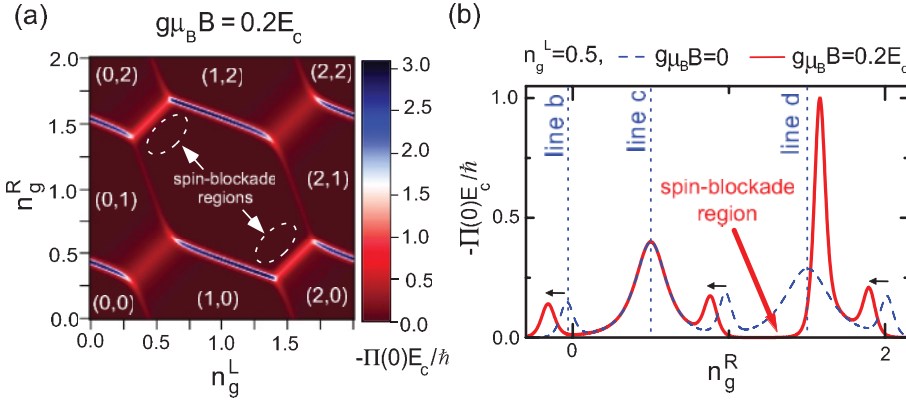
FIG. 3. (Color online) Effect of a Zeeman field on $\Pi(0)$. We have used $g\mu_B B = 0.2E_c$ for panel (a) and the red full line in panel (b), and $g\mu_B B = 0$ for the blue dashed line in panel (b). The other parameters are the same as in Fig. 2(b).

different number of states. For $\omega \gg \Gamma_{L(R)}$, using a master equation approach, we find $\Pi(\omega) \simeq -\Pi(0)\Delta_{c(d)}^2/(\omega^2 - \Delta_{c(d)}^2)$ along line $c(d)$. The finite frequency behavior of $\Pi(\omega)$ will be discussed in a more complete way elsewhere.

We now discuss the effect of a Zeeman field B on $\Pi(0)$ (see Fig. 3). We use $B > 0$ so that $\uparrow$ spins have a lower energy. Lines of type a or b are shifted by B because they now correspond essentially to a transfer of $\uparrow$ spins between the dots and leads. However, their height is almost not modified (except too close to triple points). For a magnetic field $g\mu_B B \sim t$, $\Pi(0)$ cancels in a region where line d was formerly extending [see Fig. 3(b)]. This is because in this area, the state $(\uparrow, \uparrow)$ becomes the most stable state, and therefore charge fluctuations between the two dots become impossible. This effect represents a near-equilibrium version of Pauli spin blockade.[20] As a result, line d is shifted to higher (lower) values of n_g^R (n_g^L), and it reaches a higher maximum which depends strongly on T. Indeed, we obtain for $g\mu_B B \ll E_c^{L(R)}, U_m$

$$\frac{-\Pi(0)}{\hbar(\alpha_L - \alpha_R)^2} \simeq \frac{8t^2 + e^{-\beta(\Lambda - g\mu_B B)}\left(\Delta_d^2\Lambda\beta + 2t^2(2 - \Delta_d\beta)\right)}{\Delta_d^3\{1 + \exp[\beta(\Lambda - g\mu_B B)]\}^2} \quad (9)$$

with $\Lambda = (E_{11} - E_{20} + \Delta_d)/2$. In contrast, line c is not affected by a magnetic field $g\mu_B B \sim t$. Line c is affected by B once $(\uparrow, \uparrow)$ becomes the most stable state near $n_g^R = n_g^L = 0.5$, which occurs only for higher values of magnetic field $g\mu_B B \sim U_m$ (not shown).

To conclude this first part, mesoscopic admittance measurements appear as an interesting alternative to charge sensing[12,25] for performing the spectroscopy of quasiclosed multi-quantum-dot systems. We have mainly discussed the $\Gamma_{L(R)} \ll k_B T$ limit. The frontiers between the different (n_L, n_R) domains can be seen in $\Pi(0)$. In the interacting case, the parity of the DQD total occupation number can be determined directly from the difference of amplitude between lines of type c and d obtained at $B = 0$, or from the spin blockade effect obtained for $B \neq 0$. The DQD mesoscopic admittance also gives a direct access to information on the DQD spin state, since spin singlet and triplet states can be discriminated using spin blockade. At high frequencies $\omega \sim t \gg \Gamma$, $\Pi(\omega)$ shows resonances due to the internal dynamics of the DQD. We have disregarded spin and orbital relaxation effects (with rates denoted $\Gamma_{\text{rel}}^{s/o}$), which can be due, e.g., to magnetic impurities, spin-orbit coupling, or phonons.

However, assuming $\Gamma_{\text{rel}}^{s(o)}, \Gamma_{L(R)} \ll k_B T$, the results presented here [Eqs. (7)–(9)] will not be affected for ω much smaller or much larger than $\Gamma_{\text{rel}}^{s(o)}, \Gamma_{L(R)}$. For an intermediary value of ω, the expression of $\Pi(\omega)$ can involve explicitly $\Gamma_{\text{rel}}^{s(o)}$ and $\Gamma_{L(R)}$.

We now consider an experiment where the DQD is connected through C_{ac}^L and C_{ac}^R to an external (L_r, C_r) circuit which is a simple model for a photonic resonator.[7] The full circuit Hamiltonian $\hat{H}_2$ includes terms in $(C_r/2)\hat{V}_{\text{ac}}^2 + (1/2L_r)\hat{\Phi}_{\text{ac}}^2$ and $\lambda_1\hat{V}_{\text{ac}} + \lambda_2\hat{V}_{\text{ac}}^2$ due to the resonator and DQD, respectively, with $\hat{\Phi}_{\text{ac}}$ the flux operator through the inductance L_r and $\hat{V}_{\text{ac}}$ the operator associated to V_{ac}. We define the charge operator conjugated to $\hat{\Phi}_{\text{ac}}$ as $\hat{Q}_{\text{ac}} = \hat{V}_{\text{ac}}/C_r'$ with $C_r' = C_r + 2\lambda_2$ and the photon annihilation operator $\hat{a} = -i/\sqrt{2\hbar Z_r}\hat{\Phi}_{\text{ac}} + \sqrt{Z_r/2\hbar}\hat{Q}_{\text{ac}}$ with $Z_r = \sqrt{L_r/C_r'}$. We assume that the resonator photons are coupled to an external photonic bath corresponding to the annihilation operator $\hat{b}$.[26] We finally have

$$\hat{H}_2 = \hat{H}_{\text{DQD}} + eV_{\text{rms}}\sum_d \alpha_d \hat{n}_d(\hat{a} + \hat{a}^\dagger) + \lambda_1 V_{\text{rms}}(\hat{a} + \hat{a}^\dagger)$$
$$+ \hbar\omega_r'\hat{a}^\dagger\hat{a} + \sum_p \hbar\omega_p \hat{b}_p^\dagger\hat{b}_p + \sum_p(\tau\hat{b}_p^\dagger\hat{a} + \tau^*\hat{a}^\dagger\hat{b}_p)$$
$$+ (\kappa\hat{a}e^{i\omega_d t} + \kappa^*e^{-i\omega_d t}\hat{a}^\dagger) + \hat{H}_l \quad (10)$$

with $\omega_r' = 1/\sqrt{L_r C_r'}$ and $V_{\text{rms}} = \sqrt{\hbar\omega_r'/2C_r'}$. The terms in κ account for an external driving of the resonator at frequency $\omega_d/2\pi$.[27] For simplicity, we study the response of the resonator through its mean voltage. The linear-response theory gives $\Delta V_{\text{ac}}(t) = \text{Re}[G_{\hat{a}+\hat{a}^\dagger,\hat{a}^\dagger}(\omega_d)\kappa^*e^{-i\omega_d t}]$ with $G_{\hat{A},\hat{B}}(t) = -i\theta(t)\langle[\hat{A}(t),\hat{B}]\rangle_{\kappa=0}$. We can relate $G_{\hat{a}^\dagger,\hat{a}}$ and $G_{\hat{a}^\dagger,\hat{a}^\dagger}$ to $\tilde{\chi}_{d,d'}(t) = -i\theta(t)\langle[\hat{n}_d(t),\hat{n}_{d'}]\rangle$ by using an equations of motion approach, which takes into account the stationarity of $G_{\hat{a}^\dagger[\hat{a}],\hat{a}^\dagger}$. We assume that the self-energy terms $\sum_p |\tau_p|^2/(\hbar\omega \pm \hbar\omega_p + i0^+)$ due to the coupling to the outer photon bath write $-i\hbar\Lambda$, with $\Lambda > 0$, to account simply for the finite quality factor of the resonator. We obtain the exact relation $G_{\hat{a}^\dagger,\hat{a}}(\omega) = G_0 + G_0\omega_{\text{rms}}^2\tilde{\Pi}(\omega)G_0$ with $G_0 = (\omega - \omega_r' + i\Lambda)^{-1}$, $\tilde{\Pi}(\omega) = \sum_{d,d'}\alpha_d\alpha_{d'}\tilde{\chi}_{d,d'}(\omega)$ and $\omega_{\text{rms}} = V_{\text{rms}}e/\hbar$. Using an analogous expression for $G_{\hat{a},\hat{a}^\dagger}$ and assuming $\Lambda \ll \omega_r'$, one finds $G_{\hat{a}+\hat{a}^\dagger,\hat{a}^\dagger} \simeq G_{\hat{a},\hat{a}^\dagger}$. To find the poles of $G_{\hat{a},\hat{a}^\dagger}$, a self-consistent approach is necessary.[28,29] We postulate a RPA-like approximation $G_{\hat{a},\hat{a}^\dagger}(\omega) = G_0 + G_0\omega_{\text{rms}}^2\Pi(\omega)G_{\hat{a},\hat{a}^\dagger}(\omega)$, which yields

$$G_{\hat{a},\hat{a}^\dagger}^{-1}(\omega) = G_0^{-1} - \omega_{\text{rms}}^2\Pi(\omega). \quad (11)$$

In the limit where $\hbar\omega_r'$ and $\hbar\omega_{\rm rms}^2\Pi(0)$ are both much smaller than the energy scales involved in the DQD dynamics, Eq. (11) gives a dispersive shift of the photonic resonance frequency, i.e., $\omega_r^{\rm tot} \simeq \omega_r' + \omega_{\rm rms}^2\Pi(0)$. This result can be recovered by considering a classical parallel (L_r, C_r) circuit in parallel with a capacitance $2\lambda_2 - (e^2/\hbar)\Pi(0)$ following from Eq. (3). Indeed, assuming $\omega_{\rm rms}^2\Pi(0) \ll \omega_r'$, we expect free oscillations with a frequency $\{L_r[C_r' - (e^2/\hbar)\Pi(0)]\}^{-1/2} \simeq \omega_r^{\rm tot}$. For larger values of ω_r', in the general case, the response of the resonator is not simply given by $\Pi(\omega_r')$ but by the functional form of $\Pi(\omega)$ [and thus $G(\omega)$]. For instance, let us use the resonant form $\Pi(\omega) \simeq \Omega/(\omega^2 - \Delta^2)$ obtained previously. One expects an anticrossing effect when the photonic resonator becomes resonant with the DQD. From Eq. (11), we indeed obtain $\omega_{r,\pm}^{\rm tot} = (\Delta + \omega_r')/2 \pm \sqrt{A + (\Delta - \omega_r')^2/4}$ with $A = (\Omega\omega_{\rm rms}^2)/(\Delta + \omega_r')$.

In the noninteracting case, the RPA-like approximation of $G_{\hat{a},\hat{a}^\dagger}$ can be justified by using a standard diagrammatic perturbation theory in $\alpha_{L(R)}$. For each order in $\alpha_{L(R)}$, the contribution to $G_{\hat{a},\hat{a}^\dagger}$ corresponding to a series of "bubble" diagrams must be dominant. In principle, an estimation of diagrams at fourth order in $\alpha_{L(R)}$ already provides a good indication on the validity of the RPA scheme.[30] From a dimensional analysis, the RPA-like development of $G_{\hat{a},\hat{a}^\dagger}$ is valid at least in the regime $T = 0$ with $\Lambda, E_\pm, \hbar\omega_r', \hbar\omega_r^{\rm tot} - \hbar\omega_r' \ll \Gamma$. Considering the relevance of the results given by Eq. (11), the RPA scheme is probably valid in a much wider range of parameters. However, from the fourth-order diagrams, it seems crucial to have $\omega_r^{\rm tot} - \omega_r'$ and Λ small, and Γ finite, this assertion being difficult to define quantitatively in the general case.[31]

As a conclusion for this second part, we have discussed the behavior of a high finesse photonic resonator coupled to a DQD. When photonic correlation functions can be developed along a RPA-like scheme, both the dispersive and resonant behaviors of the resonator reveal information on the DQD admittance.

[1] G. Platero and R. Aguado, Phys. Rep. **395**, 1 (2004).

[2] J. Gabelli *et al.*, Science **313**, 499 (2006); G. Fève *et al.*, *ibid.* **316**, 1169 (2007).

[3] M. Büttiker, H. Thomas, and A. Prêtre, Phys. Lett. A **180**, 364 (1993); A. Prêtre, H. Thomas, and M. Büttiker, Phys. Rev. B **54**, 8130 (1996).

[4] S. E. Nigg, R. Lopez, and M. Büttiker, Phys. Rev. Lett. **97**, 206804 (2006); Z. Ringel, Y. Imry, and O. Entin-Wohlman, Phys. Rev. B **78**, 165304 (2008).

[5] Y. Hamamoto, T. Jonckheere, T. Kato, and T. Martin, Phys. Rev. B **81**, 153305 (2010); C. Mora and K. Le Hur, Nat. Phys. **6**, 697 (2010).

[6] J. Splettstoesser, M. Governale, J. Konig, and M. Buttiker, Phys. Rev. B **81**, 165318 (2010).

[7] A. Blais, R. S. Huang, A. Wallraff, S. M. Girvin, and R. J. Schoelkopf, Phys. Rev. A **69**, 062320 (2004).

[8] A. Wallraff *et al.*, Nature (London) **431**, 162 (2004).

[9] M. A. Sillanpää, T. Lehtinen, A. Paila, Y. Makhlin, L. Roschier, and P. J. Hakonen, Phys. Rev. Lett. **95**, 206806 (2005); T. Duty, G. Johansson, K. Bladh, D. Gunnarsson, C. Wilson, and P. Delsing, *ibid.* **95**, 206807 (2005).

[10] A. Wallraff *et al.*, Nature (London) **431**, 162 (2004).

[11] J. R. Petta *et al.*, Science **309**, 2180 (2005).

[12] H. O. H. Churchill, F. Kuemmeth, J. W. Harlow, A. J. Bestwick, E. I. Rashba, K. Flensberg, C. H. Stwertka, T. Taychatanapat, S. K. Watson, and C. M. Marcus, Phys. Rev. Lett. **102**, 166802 (2009).

[13] G. Burkard, D. Loss, and D. P. di Vincenzo, Phys. Rev. B **59**, 2070 (1999).

[14] T. Hayashi, T. Fujisawa, H. D. Cheong, Y. H. Jeong, and Y. Hirayama, Phys. Rev. Lett. **91**, 226804 (2003).

[15] L. Childress, A. S. Sørensen, and M. D. Lukin, Phys. Rev. A **69**, 042302 (2004).

[16] A. Cottet and T. Kontos, Phys. Rev. Lett. **105**, 160502 (2010).

[17] K. D. Petersson *et al.*, Nano Lett. **10**, 2789 (2010).

[18] R.-P. Riwar and J. Splettstoesser, Phys. Rev. B **82**, 205308 (2010).

[19] R. Ziegler, C. Bruder, and Herbert Schoeller, Phys. Rev. B **62**, 1961 (2000).

[20] K. Ono *et al.*, Science **297**, 1313 (2002).

[21] W. G. van der Wiel *et al.*, Rev. Mod. Phys. **75**, 1 (2002).

[22] We use $E_c^{L(R)} = C_\Sigma^{R(L)}e^2/2D$, $U_m = C_m e^2/D$, $D = C_\Sigma^L C_\Sigma^R - C_m^2$, $\alpha_{L(R)} = -(C_{\rm ac}^{L(R)}C_\Sigma^{R(L)} + C_{\rm ac}^{R(L)}C_m)/D$, $\lambda_2 = \sum_d(1 + \alpha_d)C_{\rm ac}^d/2$, $C_\Sigma^d = C_{\rm ac}^d + C_g^d + C_r^d + C_m$. We use $e > 0$ and $A(\omega) = \int_{-\infty}^{+\infty}A(t)\exp(i\omega t)dt$.

[23] In the noninteracting limit, one must assume that geometric capacitances have a negligible contribution to $G(\omega) \simeq i\omega(e^2/\hbar)\Pi(\omega)$. In principle, one can account for geometric capacitances by treating $\hat{H}_{\rm DQD}$ at the Hartree level (Ref. 3). In the Coulomb-blockade limit, our treatment fully takes into account geometric capacitances.

[24] We note (s_L, s_R) a DQD charge state with dot $d \in \{L, R\}$ in the occupation state $s_d \in \{0, 1, 2\}$, or $\{0, \uparrow, \downarrow, \uparrow\downarrow\}$ if the spin state is specified.

[25] J. M. Elzerman *et al.*, Nature (London) **430**, 431 (2004); Y. Hu *et al.*, Nat. Nanotechnol. **2**, 622 (2007).

[26] A. A. Clerk *et al.*, Rev. Mod. Phys. **82**, 1155 (2010).

[27] A. Blais, J. Gambetta, A. Wallraff, D. I. Schuster, S. M. Girvin, M. H. Devoret, and R. J. Schoelkopf, Phys. Rev. A **75**, 032329 (2007).

[28] A perturbative treatment at lowest order in $\alpha_{L(R)}$ would give the absurd result $\omega = \omega_r'$.

[29] J. Skoldberg, T. Lofwander, V. S. Shumeiko, and M. Fogelstrom, Phys. Rev. Lett. **101**, 087002 (2008).

[30] D. F. Urban, R. Avriller, and A. Levy Yeyati, Phys. Rev. B **82**, 121414 (2010).

[31] If the photon and electron linewidths Λ and Γ both vanish, all fourth-order diagrams diverge like $(\omega - \omega_r')^{-3}$. If Γ remains finite while Λ vanishes, the double bubble diagram (DBD) keeps a divergence in $(\omega - \omega_r')^{-3}$, while the others diverge like $(\omega - \omega_r')^{-2}$. Therefore we expect that for Γ sufficiently large, and Λ and $\omega_r^{\rm tot} - \omega_r'$ sufficiently small, the DBD will be the dominant fourth-order contribution to $G_{\hat{a},\hat{a}^\dagger}^{-1}(\omega_r^{\rm tot})$.